ACS Macro Letters

Letter

pubs.acs.org/macroletters

Highly-Tunable Polymer/Carbon Nanotubes Systems: Preserving Dispersion Architecture in Solid Composites via Rapid Microfiltration

Guy Mechrez,[†] Ran Y. Suckeveriene,[†] Evgeni Zelikman,[†] Jasmine Rosen,[†] Nava Ariel-Sternberg,[‡] Rina Cohen,[‡] Moshe Narkis,*[,†] and Ester Segal*[,§,∥]

[†]Department of Chemical Engineering, [§]Department of Biotechnology and Food Engineering, and [∥]The Russell Berrie Nanotechnology Institute, Technion−Israel Institute of Technology, Haifa 32000, Israel

[‡]Elbit Systems Electro-Optics-Elop Ltd., Advanced Technology Park, Rehovot 76111, Israel

Supporting Information

ABSTRACT: This research presents a new fabrication method for tailoring polymer/carbon nanotube (CNT) nanostructures with controlled architecture and composition. The CNTs are finely dispersed in polymeric latex, that is, polyacrylate, via ultrasonication, followed by a microfiltration process. The latter step allows preserving the homogeneous dispersion structure in the resulting solid nanocomposite. The combination of microfiltration and proper choice of the polymer latex, particle size, and composition allows the design of complex nanostructures with tunable properties, for example, porosity and mechanical properties. An important attribute of this methodology is the ability to tailor any desired composition of polymer−CNT systems, that is, nanotube content can practically vary anywhere between 0 to 100 wt %. Thus, for the first time, a given polymer/CNT system is studied over the entire CNTs composition, resembling two-phase polymer blends. The polyacrylate in these systems exhibits a structural transition from a continuous matrix (nanocomposite) to segregated domains dispersed within a porous CNTs network. An analogy of this structural transition to phase inversion phenomena in two-phase polymer blends is suggested. The resulting polyacrylate/CNT layers exhibit a percolation threshold as low as 0.04 wt %. Additionally, these nanomaterials show low total reflectance values throughout the visible, NIR and SWIR spectrum at a CNT content as low as 1 wt %, demonstrating their potential applicability for optical devices.

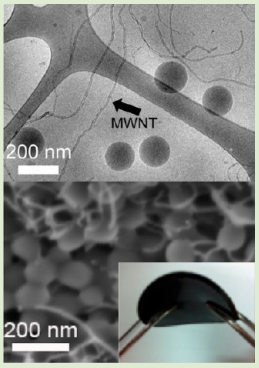

An immense research effort has been directed toward the development of polymer/carbon nanotube (CNT) systems and nanocomposites.[1−4] The combination of CNTs with polymers offers an attractive route for introducing new functionalities to the resulting materials, based on their morphological modification and the interaction between the two components.[5−7] A straightforward approach for the fabrication of polymer/CNT nanocomposites is based on dispersing the nanotubes within an aqueous polymeric dispersion.[8−19] The polymer dispersion is usually synthesized by emulsion polymerization (e.g., of styrene or acrylate monomers) and is commonly termed as a latex. This fabrication process involves the predispersion of CNTs in an aqueous surfactant solution by ultrasonication or high-shear mixing. The resulting CNT dispersion is mixed with a given polymer latex, followed by evaporation of the aqueous phase (e.g., via freeze- or vacuum-drying), which leads to the coalescence of the polymer nano/micro particles (above the glass transition temperature, T_g, of the polymer). These polymer/CNT nanocomposites have demonstrated appealing properties for many applications, including thin films,[12] porous electrodes,[10,11] thermoelectrics,[13,18] and conductive foams.[20]

The present study introduces a rapid and facile fabrication method for tailoring polymer/CNT nanostructures with controlled architecture and composition. The CNTs are finely dispersed in a polyacrylate latex via ultrasonication, followed by a microfiltration process. The latter step allows preserving the homogeneous dispersion structure in the resulting solid nanocomposite. An important attribute of this methodology is the ability to tailor any desired composition of polymer−CNT systems, that is, nanotube content can practically vary anywhere between 0 and 100 wt %. Thus, for the first time a given polymer/CNTs system is studied over the entire CNTs composition range.

Recent studies have shown that CNTs exhibit similar characteristics to those of rigid polymer molecules.[21−23] Based on this new perspective, conceptually considering CNTs as rigid macromolecules, polymer/CNT systems can be considered as two-phase polymer blends. Thus, our method enables the design of any desired composition of the two components similar to binary two-phase polymer blends. We demonstrate this new concept in polyacrylate/multiwalled carbon nanotubes (MWNTs) systems. The morphology, electrical and optical properties of the resulting polyacrylate/MWNTs nanomaterials are investigated. We show that upon increasing nanotubes content a structural transition is observed; from dispersed nanotube domains into a continuous CNT porous matrix. An analogy of this structural transition to phase

Received: March 27, 2012
Accepted: June 13, 2012
Published: June 19, 2012

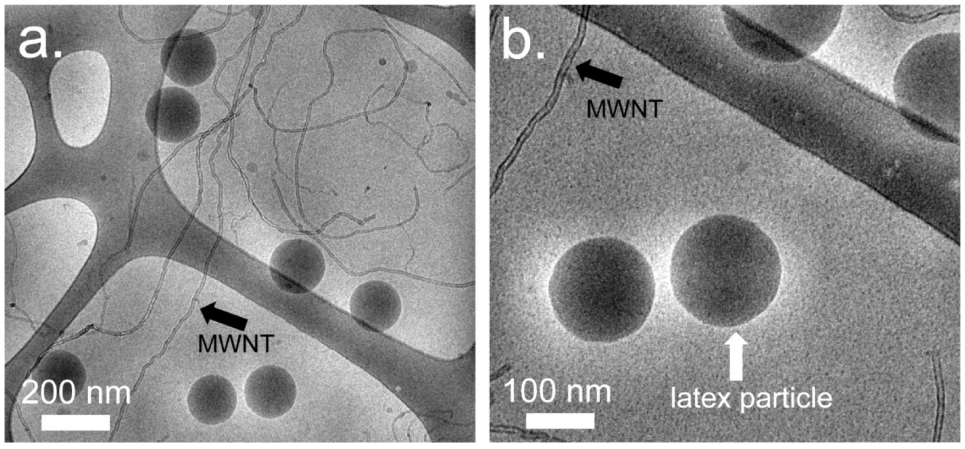

Figure 1. Cryo-TEM micrographs of polyacrylate/MWNTs dispersion (latex to MWNTs ratio is 4:1): (a) low and (b) high magnification. Black arrows depict individually dispersed MWNTs; white arrow depicts polyacrylate latex nanoparticle. Spherical DBSA micelles are observed at the background.

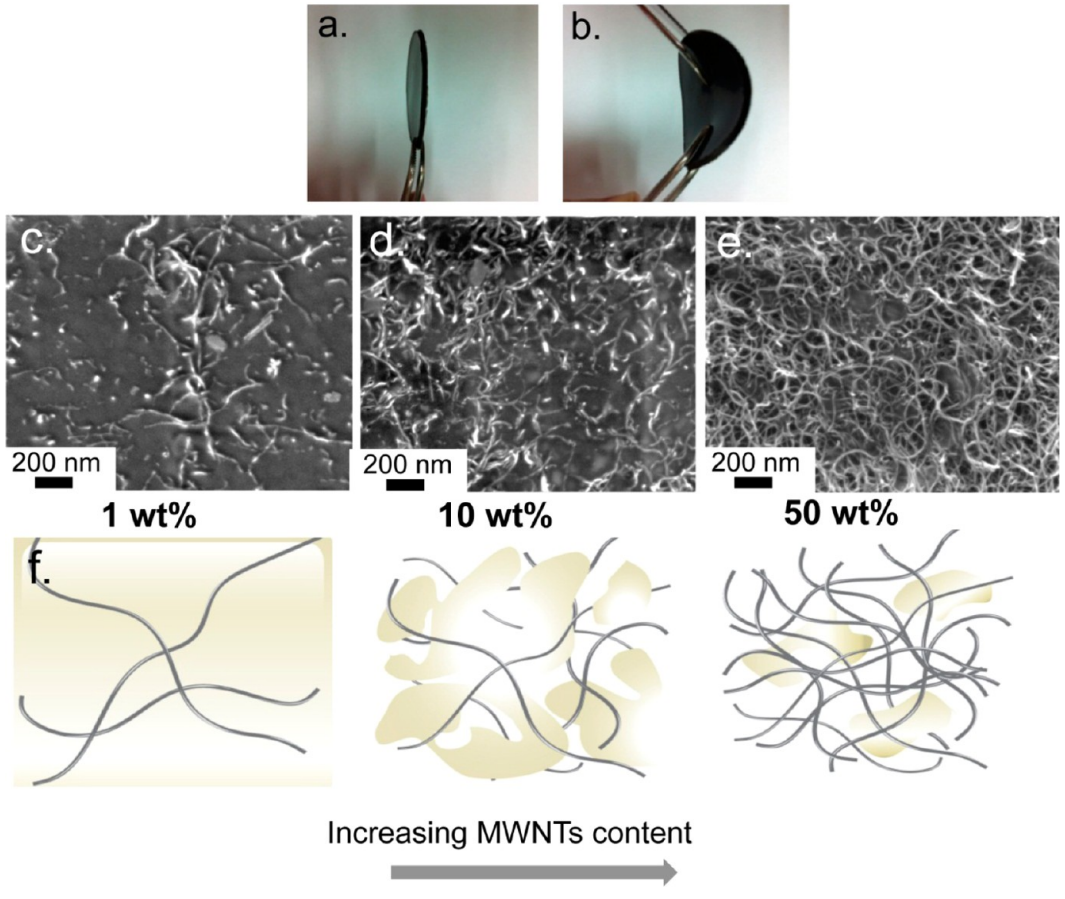

Figure 2. Images of a typical solid polyacrylate/MWNTs layer (300 μm in thickness and 35 mm in diameter), demonstrating its integrity and flexibility; the layer contains 5 wt % MWNT (a, b). High-resolution SEM micrographs of solid polyacrylate/MWNTs layers of different MWNTs content: (c) 1 wt %, (d) 10 wt %; (e) 50 wt % MWNT. The polyacrylate latex has a T_g of 19 °C (B.G polymers, Israel). A schematic illustration of the polyacrylate/MWNT layers nanostructure at nanotubes content ranging from 1 to 50 wt %, corresponding to the morphology observed by SEM (f).

inversion phenomena in two-phase polymer blends is suggested.

MWNTs (Nanocyl 7000, Belgium; diameter of ~9.5 nm and length of ~1.5 μm; carbon purity 90 wt % and metal oxide 10 wt %) are dispersed in a polyacrylate latex (B.G polymers, Israel, see details in the Supporting Information) together with an aqueous dodecylbenzene sulfonic acid, DBSA (Zohar Dalia, Israel) solution by ultrasonication (Vibra cell VCX 750 - Sonics and Materials Inc., U.S.A.). The MWNT/DBSA weight ratio is kept constant at 1:5 in all samples. The nanostructure of the resulting aqueous dispersions is characterized via direct imaging using cryo-transmission electron microscopy (cryo-TEM). TEM micrographs are obtained for ultrafast cooled vitrified cryo-TEM specimens prepared under controlled conditions of

dx.doi.org/10.1021/mz300145a | *ACS Macro Lett.* 2012, 1, 848−852

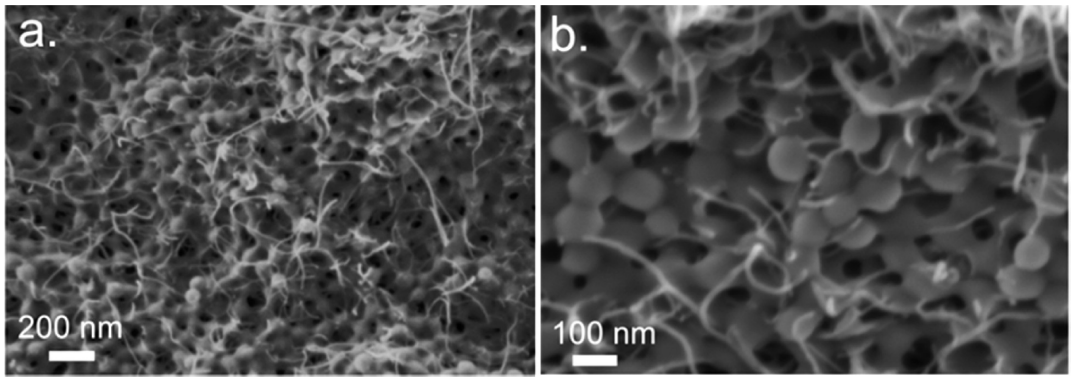

Figure 3. High-resolution SEM micrographs of a solid polyacrylate/MWNT layer containing 5 wt % MWNTs at (a) low and (b) high magnification. The polyacrylate latex has a T_g of 35 °C.

20 °C and 100% relative humidity, as described elsewhere.[24] Specimens are examined in a Philips CM120 cryo-TEM operating at 120 kV, using an Oxford CT3500 cooling-holder system at about −180 °C. Low electron-dose imaging is performed with a Gatan Multiscan 791 CCD camera, using the Gatan Digital Micrograph 3.1 software package. Cryo-TEM images of a typical polyacrylate/MWNTs system (latex to MWNTs ratio is 4:1) show that the nanotubes and the polyacrylate nanoparticles (~100 nm in diameter) form a homogeneous dispersion in which both components are individually dispersed (Figure 1).

The polyacrylate/MWNTs dispersions are subsequently filtered through a microporous hydrophilic membrane (mixed cellulose ester membranes 0.45 μm and a diameter of 47 mm, Millipore LTD, Ireland) under vacuum, as depicted in Figure S1 (see Supporting Information). During the microfiltration process, both the CNTs and the polyacrylate nanoparticles accumulate on the membrane. The thickness of the layer can be adjusted and herein is tuned to 300 ± 10 μm. The resulting layer is easily removed from the support and dried overnight at room temperature, leaving a free-standing film. Several polyacrylate/MWNT systems are fabricated; the MWNT content in the dry solid layers is 0, 0.05, 0.2, 1, 5, 10, 20, 30, 50, and 100 wt %.

Figure 2a,b shows images of a typical polyacrylate/MWNTs layer, demonstrating its integrity and flexibility. The morphology of the resulting layers was studied using LEO 982 (Cambridge, U.K.) scanning electron microscope (SEM) equipped with a high-resolution field emission gun (FEG), operating at a 4 kV accelerating voltage and a 3−4 mm working distance, and an in-lens detector of secondary electrons. High-resolution SEM micrographs of polyacrylate/MWNT layer containing 1, 10, and 50 wt % MWNTs are shown in Figure 2c, d, and e, respectively. At a concentration of 1 wt % MWNTs, uniformly dispersed nanotubes are observed within the continuous polyacrylate matrix, forming a delicate network (Figure 2c). The polyacrylate used in this study has a T_g of 19 °C (determined by dynamic mechanical thermal analysis, data not shown). Thus, the formation of a continuous polyacrylate matrix arises from the coalescence of the latex nanoparticles at room temperature. At a high MWNTs content of 50 wt %, the nanotubes form a porous "matrix" and the coalesced polyacrylate acts as the dispersed phase (Figure 2e). A "phase inversion" is observed at MWNTs content around 10 wt %, (Figure 2d). In analogy to two-phase polymer blends, at this concentration range, the MWNTs and the polyacrylate are forming cocontinuous phases. At this MWNT concentration range, a structural transition is observed, that is, from nanotubes dispersed within a polymer matrix (nanocomposite) into a continuous MWNT porous matrix, in which segregated coalesced polyacrylate domains are entrapped, as schematically illustrated in Figure 2f.

The presented fabrication method allows us to tailor and control the resulting nanostructure by varying the T_g of the latex. Figure 3 depicts cross-sectional SEM micrographs of a polyacrylate(T_g = 35 °C)/MWNT layer containing 5 wt % MWNTs. As the T_g of the polyacrylate is above room temperature, only minor coalescence of the latex nanoparticles is observed. These layers exhibit nanoscale pores (20−80 nm), resulting from the partial coalescence ability of the polymer particles. Furthermore, this system provides an insight as for the formation mechanism of the layers during the microfiltration process. The uniform dispersion of the nanotubes in between the latex nanoparticles, observed in Figure 3b, is preserved during the microfiltration process. Achieving a high degree of nanotubes dispersion in a polymer matrix is difficult to attain using common methods, for example, solution-casting processes,[17,25] due to the strong agglomeration tendency of the CNTs.

The microfiltration process also maintains the original dispersion composition in the final solid layer. Table 1 compares the content of polyacrylate and MWNTs in the aqueous dispersion to that of the resulting solid layers, as determined by thermal gravimetric analysis in air (TA Instruments 2050 TGA). The significant difference in the

Table 1. Composition of Polyacrylate/MWNT Aqueous Dispersions Compared to the Composition of the Resulting Dried Solid Layer Obtained by Microfiltration (as Determined by TGA)

polyacrylate content in aqueous dispersion[a] (wt%)	polyacrylate content in solid layer (wt%)	MWNT content in aqueous dispersion[a] (wt%)	MWNT content in solid layer (wt%)
99 ± 0.5	99 ± 0.3	1 ± 0.5	1 ± 0.3
95 ± 0.5	95 ± 0.3	5 ± 0.5	5 ± 0.3
90 ± 0.5	90 ± 0.3	10 ± 0.5	10 ± 0.3
80 ± 1	82 ± 0.5	20 ± 1	17 ± 0.5
70 ± 1	74 ± 0.5	30 ± 1	26 ± 0.5
50 ± 1	63 ± 0.5	50 ± 1	37 ± 0.5

[a]Note that MWNT and polyacrylate concentrations in the dispersions are calculated on a dry basis.

dx.doi.org/10.1021/mz300145a | ACS Macro Lett. 2012, 1, 848−852

thermal decomposition temperatures of polyacrylate and MWNTs (300 and 600 °C, respectively) allows us to precisely calculate the composition of the layers. The results in Table 1 show that there are only minor differences in the composition of the original dispersion in comparison to that of the solid layers. At MWNT content higher than 30 wt % (on a dry basis), the discrepancy between the dispersion composition and the resulting solid layer tends to increase due to CNT loss at the initial microfiltration stage in which the nanotubes accumulate on the membrane and form the porous bed. In addition, the TGA studies show that the solid layers are free of surfactant (see Figure S2, Supporting Information), confirming that the DBSA is removed during the microfiltration process.

Figure 4 depicts the volume electrical conductivity of the polyacrylate/MWNT systems. A four-point probe technique is

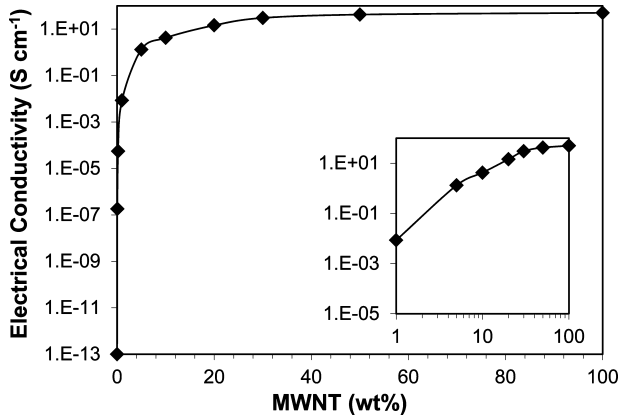

Figure 4. Electrical conductivity of polyacrylate/MWNT layers versus MWNTs content.

used to measure the electrical conductivity of the layers (at values higher than 10^{-4} S/cm). For conductivity values lower than 10^{-4} S/cm, a two-point method is applied. The percolation threshold is observed at a MWNTs content of 0.04 wt %. This value is significantly lower in comparison to other polymer/MWNTs systems reported in the literature.[25−30] The obtained low percolation threshold is attributed to the dispersion uniformity of the MWNTs within the polyacrylate matrix, as observed in Figure 2. Above percolation, the studied systems exhibit a further conductivity increase of more than 1 order of magnitude as MWNTs content is increased from 10 to 50 wt % (inset Figure 4). It should be emphasized that this behavior is not a common behavior in percolative conductive systems in general,[31−34] and in polymer/CNTs nanocomposites in particular.[35−37] However, this behavior may be observed in segregated network composites in which weak matrix−filler interaction allows for intimate contact among the nanotubes. We ascribe this finding to the resemblance of our highly filled polymer (e.g., 50 wt % MWNTs) to Bucky paper systems.[38−40] To the best of our knowledge, this is the first time that the electrical conductivity of a polymer/CNTs system, which is fabricated under the same conditions, is presented and characterized over the entire CNT concentration range (0 to 100 wt % CNTs).

To demonstrate the potential applicability of the polyacrylate/MWNT layers as low reflectance films, we have measured their total reflectance over a broad range of wavelengths, from visible through near IR (NIR) to short-wavelength IR (SWIR). The films total reflectance at a wavelength range of 400−2000 nm is characterized by a Jasco 570 spectrophotometer, with an integrating sphere. The system consists of two detectors, which are switched automatically, a photomultiplier detector for the UV−visible and a Peltier-cooled PbS detector for the NIR-SWIR range. The background is measured with a white reference and the total reflectance of the sample is normalized and compared to a 100% reflecting background. Pure polyacrylate layer is transparent and is showing reflectance identical to the white reference. Layers of three different polyacrylate/MWNT systems (1, 10, and 30 wt % MWNTs) exhibit a decreasing total reflectance value in the visible range reaching values as low as ∼4% throughout the NIR and the SWIR wavelength range. It should be noted that the total reflectance of the 1 wt % MWNT layer is lower in comparison to systems containing higher CNTs contents. We assign this behavior to the high dispersion level of the MWNTs within the polyacrylate matrix, achieved by the microfiltration fabrication method. Moreover, using latex nanoparticles as the major component (99 wt %), allows for facile application of these layers, as their adhesion and mechanical properties are highly tunable. The latex type and the resulting layer properties can be tailored to meet the requirements of the desired performance.

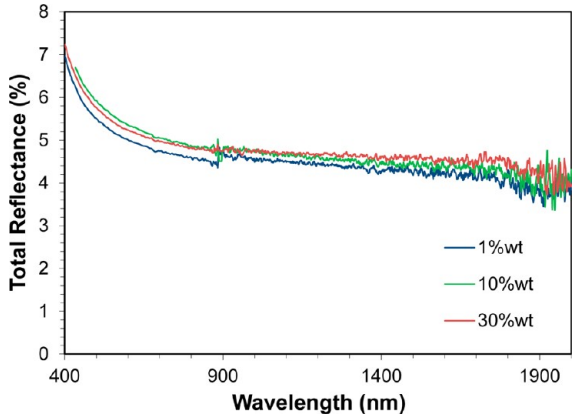

Figure 5. Total reflectance of three different polyacrylate/MWNT systems (1, 10, and 30 wt % MWNTs) as a function of the wavelength of the incident radiation (from visible through near IR to short-wavelength IR).

This research presents a new fabrication method of polymer/CNT systems based on microfiltration of latex and MWNT dispersions. We show that this methodology allows for the design of polymer/CNT layers at any desired composition, that is, nanotubes concentration can practically range from 0 to 100 wt %, resembling two-phase polymer blends. The polyacrylate phase in these systems exhibits a structural transition from a continuous matrix (nanocomposite) to segregated domains dispersed within a porous CNTs network. An analogy of this structural transition to phase inversion phenomena in a two-phase polymer blend is suggested. The resulting polyacrylate/MWNT layers exhibit a percolation threshold as low as 0.04 wt % MWNT. Additionally, these nanomaterials show low total reflectance values throughout the visible, NIR and SWIR spectrum at a CNT content as low as 1 wt %, demonstrating their potential applicability for optical devices. The combination of microfiltration and proper choice of the polymer latex, particle size, and composition allows the design of complex architectures with tunable properties.

dx.doi.org/10.1021/mz300145a | ACS Macro Lett. 2012, 1, 848−852

■ ASSOCIATED CONTENT

Supporting Information

Additional experimental details and figures. This material is available free of charge via the Internet at http://pubs.acs.org.

■ AUTHOR INFORMATION

Corresponding Author

*E-mail: narkis@tx.technion.ac.il; esegal@tx.technion.ac.il.

Notes

The authors declare no competing financial interest.

■ ACKNOWLEDGMENTS

The financial support of the Russell Berrie Nanotechnology Institute is gratefully acknowledged. This work was partially supported by the Magnet program, administered by the Israel Ministry of Trade and Industry, NES consortium.

■ REFERENCES

(1) Grossiord, N.; Loos, J.; Regev, O.; Koning, C. E. *Chem. Mater.* **2006**, *18* (5), 1089−1099.

(2) Grossiord, N.; Loos, J.; van Laake, L.; Maugey, M.; Zakri, C.; Koning, C. E.; Hart, A. J. *Adv. Funct. Mater.* **2008**, *18* (20), 3226−3234.

(3) Moniruzzaman, M.; Winey, K. I. *Macromolecules* **2006**, *39* (16), 5194−5205.

(4) Breuer, O.; Sundararaj, U. *Polym. Compos.* **2004**, *25* (6), 630−645.

(5) Zhang, D.; Ryu, K.; Liu, X.; Polikarpov, E.; Ly, J.; Tompson, M. E.; Zhou, C. *Nano Lett.* **2006**, *6* (9), 1880−1886.

(6) Choi, W.; Ohtani, S.; Oyaizu, K.; Nishide, H.; Geckeler, K. E. *Adv. Mater.* **2011**, *23* (38), 4440−4443.

(7) Goldman, D.; Lellouche, J.-P. *Carbon* **2010**, *48* (14), 4170−4177.

(8) Antonietti, M.; Shen, Y.; Nakanishi, T.; Manuelian, M.; Campbell, R.; Gwee, L.; Elabd, Y. A.; Tambe, N.; Crombez, R.; Texter, J. *ACS Appl. Mater. Interfaces* **2010**, *2* (3), 649−653.

(9) Cai, D.; Song, M. *Carbon* **2008**, *46* (15), 2107−2112.

(10) Das, R. K.; Liu, B.; Reynolds, J. R.; Rinzler, A. G. *Nano Lett.* **2009**, *9* (2), 677−683.

(11) Dionigi, C.; Stoliar, P.; Ruani, G.; Quiroga, S. D.; Facchini, M.; Biscarini, F. *J. Mater. Chem.* **2007**, *17* (35), 3681−3686.

(12) Kara, S.; Arda, E.; Dolastir, F.; Pekcan, O. *J. Colloid Interface Sci.* **2010**, *344* (2), 395−401.

(13) Kim, D.-Y.; Kim, Y.-S.; Choi, K.-W.; Grunlan, J. C.; Yu, C.-H. *ACS Nano* **2010**, *4* (1), 513−523.

(14) Masenelli-Varlot, K.; Chazeau, L.; Gauthier, C.; Bogner, A.; Cavaille, J. Y. *Compos. Sci. Technol.* **2009**, *69* (10), 1533−1539.

(15) Mu, M.; Walker, A. M.; Torkelson, J. M.; Winey, K. I. *Polymer* **2008**, *49* (5), 1332−1337.

(16) Park, E. J.; Hong, S.; Park, D. W.; Shim, S. E. *Colloid Polym. Sci.* **2010**, *288* (1), 47−53.

(17) Regev, O.; ElKati, P. N. B.; Loos, J.; Koning, C. E. *Adv. Mater. (Weinheim, Ger.)* **2004**, *16* (3), 248−251.

(18) Yu, C.; Kim, Y. S.; Kim, D.; Grunlan, J. C. *Nano Lett.* **2008**, *8* (12), 4428−4432.

(19) Yu, J.; Lu, K.; Sourty, E.; Grossiord, N.; Koning, C. E.; Loos, J. *Carbon* **2007**, *45* (15), 2897−2903.

(20) Hermant, M. C.; Verhulst, M.; Kyrylyuk, A. V.; Klumperman, B.; Koning, C. E. *Compos. Sci. Technol.* **2009**, *69* (5), 656−662.

(21) Green, M. J.; Behabtu, N.; Pasquali, M.; Adams, W. W. *Polymer* **2009**, *50* (21), 4979−4997.

(22) Fakhri, N.; MacKintosh Frederick, C.; Lounis, B.; Cognet, L.; Pasquali, M. *Science* **2010**, *330* (6012), 1804−7.

(23) Duggal, R.; Pasquali, M. *Phys. Rev. Lett.* **2006**, *96* (24), 246104.

(24) Talmon, Y. *Surfactant Sci. Ser.* **1999**, *83* (Modern CharacterizationMethods of Surfactant Systems), 147−178.

(25) Shaffer, M. S. P.; Windle, A. H. *Adv. Mater. (Weinheim, Ger.)* **1999**, *11* (11), 937−941.

(26) Kimura, T.; Ago, H.; Tobita, M.; Ohshima, S.; Kyotani, M.; Yumura, M. *Adv. Mater. (Weinheim, Ger.)* **2002**, *14* (19), 1380−1383.

(27) Park, S. H.; Bandaru, P. R. *Polymer* **2010**, *51* (22), 5071−5077.

(28) Zeng, Y.; Liu, P.; Du, J.; Zhao, L.; Ajayan, P. M.; Cheng, H.-M. *Carbon* **2010**, *48* (12), 3551−3558.

(29) Blanchet, G. B.; Fincher, C. R.; Gao, F. *Appl. Phys. Lett.* **2003**, *82* (8), 1290−1292.

(30) Li, J.; Ma, P. C.; Chow, W. S.; To, C. K.; Tang, B. Z.; Kim, J.-K. *Adv. Funct. Mater.* **2007**, *17* (16), 3207−3215.

(31) Cao, Q.; Song, Y.; Tan, Y.; Zheng, Q. *Polymer* **2009**, *50* (26), 6350−6356.

(32) Drubetski, M.; Siegmann, A.; Narkis, M. *J. Mater. Sci.* **2007**, *42* (1), 1−8.

(33) Shamir, D.; Siegmann, A.; Narkis, M. *J. Appl. Polym. Sci.* **2010**, *115* (4), 1922−1928.

(34) Shemesh, R.; Siegmann, A.; Tchoudakov, R.; Narkis, M. *J. Appl. Polym. Sci.* **2006**, *102* (2), 1688−1696.

(35) Zhao, Z.; Zheng, W.; Yu, W.; Long, B. *Carbon* **2009**, *47* (8), 2118−2120.

(36) Du, F.; Scogna, R. C.; Zhou, W.; Brand, S.; Fischer, J. E.; Winey, K. I. *Macromolecules* **2004**, *37* (24), 9048−9055.

(37) Wang, T.; Lei, C.-H.; Dalton, A. B.; Creton, C.; Lin, Y.; Fernando, K. A. S.; Sun, Y.-P.; Manea, M.; Asua, J. M.; Keddie, J. L. *Adv. Mater. (Weinheim, Ger.)* **2006**, *18* (20), 2730−2734.

(38) Park, J. G.; Yun, N. G.; Park, Y. B.; Liang, R.; Lumata, L.; Brooks, J. S.; Zhang, C.; Wang, B. *Carbon* **2010**, *48* (15), 4276−4282.

(39) Izadi-Najafabadi, A.; Yamada, T.; Futaba, D. N.; Yudasaka, M.; Takagi, H.; Hatori, H.; Iijima, S.; Hata, K. *ACS Nano* **2011**, *5* (2), 811−819.

(40) Cha, S. I.; Kim, K. T.; Lee, K. H.; Mo, C. B.; Jeong, Y. J.; Hong, S. H. *Carbon* **2008**, *46* (3), 482−488.